Method for Filling and Sharpening False Colour Layers of Dual Energy X-ray Images

Krzysztof Dmitruk, Michał Mazur, Marcin Denkowski, Paweł Mikołajczak

Abstract—An X-ray scanning and image processing have a vast range of applications in the security. An image of a content of some package being passed for example to an airplane or to the court house may help to figure out if there are any dangerous objects inside that package and to avoid possible threatening situation. As the raw X-ray images are not always easy to analyze and interpret, some image processing methods like an object detection, a frequency resolution increase or a pseudocolouring are being used. In this paper, we propose a pseudocoloring improvement over material based approach. By addition of the edge detection methods we fill and sharpen colour layers over the image, making it easier to interpret. We demonstrate the effectiveness of the methods using real data, acquired from a professional dual energy X-ray scanner.

Keywords—X-ray imaging, image processing, false colour, object detection.

I. Introduction

X-RAY scanners provide images based on different level of absorption of radiation of different materials. Scanners are used for example in medical tomography and security on which we focus. In most cases, the resulting images are displayed in grayscale where the most absorbing parts are colored white, and areas transparent to the rays are colored with black. Inversion of this colourspace is also popular and frequently used. This kind of presentation, in some applications, is good enough for well-trained technicians, but the necessity of providing more details to images causes that some marking is required.

A common approach is to use a linear color map. For example a cubehelix (black – blue – green – red – white) false colouring expands the depth resolution of images 5 times, see [1] and [2]. More advanced methods allow to classify scanned objects or their parts to certain materials on the basis of mass attenuation coefficient. This coefficient depends on the material's atomic number. In theory, it should allows us to classify the object on the basis of their atomic number, but tests showed, that objects' thickness has a major impact on the classification. The fire extinguisher is the example of cylindrical objects, where this effect is clearly visible (see Fig. 1c).

K. Dmitruk is with Institute of Computer Science, M.Curie-Sklodowska University, Lublin, Poland, (e-mail: krzysztof.dmitruk@umcs.lublin.pl).

M. Mazur is with Zeszuta Sp. z o.o., Radom, Poland, (e-mail: michal.mazur@zeszuta.pl).

M. Denkowski is with Institute of Computer Science, M.Curie-Sklodowska University, Lublin, Poland, (e-mail: krzysztof.dmitruk@umcs.lublin.pl).

P. Mikołajczak is with Institute of Computer Science, M.Curie-Sklodowska University, Lublin, Poland, (e-mail: krzysztof.dmitruk@umcs.lublin.pl).
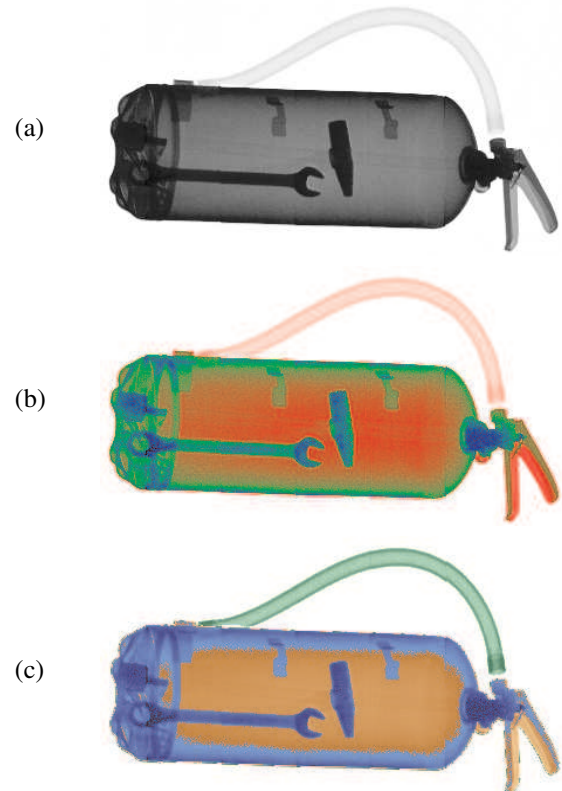
Fig. 1. Approaches of false colouring: (a) raw image, (b) linear colour mask, (c) material based colour mask.

The proposed approach is based on material qualification, but also takes objects' shapes into account. Such a structure and geometric description is used to correct object assignment. Our aim is to provide images that allow to easily distingush one object from another. The presented method is capable of colorizing that objects in a way that it matches its material. It is also important to remove the most of artifacts and unexpected transitions of material colour ranges, but preserving sharp borders between objects.

II. Methodology

An X-ray inspection system is composed of X-ray source, X-ray detector and conveyor belt, see [3]. Security scanners use a very short ($0.01 - 10$ nm) electromagnetic radiation waves called X-rays. X-rays are emitted with photon energy ranging from 30 to 200 KeV, see [4]. Photons successfully passed through a scanned object are measured by detectors ordered in a L-shaped bar, see[5]. As the baggage goes through

the scanner tunnel, the attenuated X-rays are collcted by the row of detectors. Detectors' driver assembles data from multiple detectors into one discrete grayscale image.

A. Hardware

Our scanner works with a single X-ray monoblock generator and a dual energy range detector which provides simultaneously two energy images. This means, that during one-time X-ray shot, we obtain two sets of data for two images generation (low and high energy, LE and HE respectively). The dual energy capable detector has a complicated construction. There are two scintillators, for low energy: GOS (153mg/cm2) and for high energy: CsI(TI). The first one is 3.0 mm thick and the second one is 4.1 mm thick. There is also a filter element (0.6 mm copper) between LE and HE scintillator. In order to produce our test images X-ray, tube generates rays using 160 keV voltage with 5300 μA current, which are measured by the detectors after passing through scanned objects. We are using Spellman XRB160P model/type tube with X-Scan 1,5L-1253 DE-ENET detectors.

Tested objects were moved by conveyor at 40 cm/s speed rate. Scanned objects could have maxiumum width of 1000 mm and unlimited length due to the possibility of moving them horizontally.

B. Dual energy

For our scans, we use dual energy data collection. Dual energy X-ray imaging brings us benefits in the form of depth resolution enhancement, because of slightly different attenuation characteristics which are depending on photons energy. In this section data acqustion from detectors and creation of raw images is discussed, see [6].

X-ray tube emits N_0 photons and only N passes through scanned object and reaches the detector. The numbers of photons that will pass through object depends on its attenuation (μ) and object thickness (T):

$$N = N_0 \exp(-\mu T) \tag{1}$$

The coefficient μ depends on the density of the material (ρ), and mass attenuation of the material (τ). τ is experimentally obtained and tabularized function depending on the material effective atomic number (Z) and energy of the photons (E):

$$\mu = \rho \cdot \tau(E, Z) \tag{2}$$

Attenuation graphs for some substances are displayed on figure 2.

From equation 1 we have:

$$-\log(N/N_0) = \mu T \tag{3}$$

and finally we get the following equation:

$$-\log(N/N_0) = T \cdot \rho \cdot \tau(E, Z) = m_E \tag{4}$$

which means, there is proportion between number of rays that crossed a scanned object and coefficient of its attenuation. If
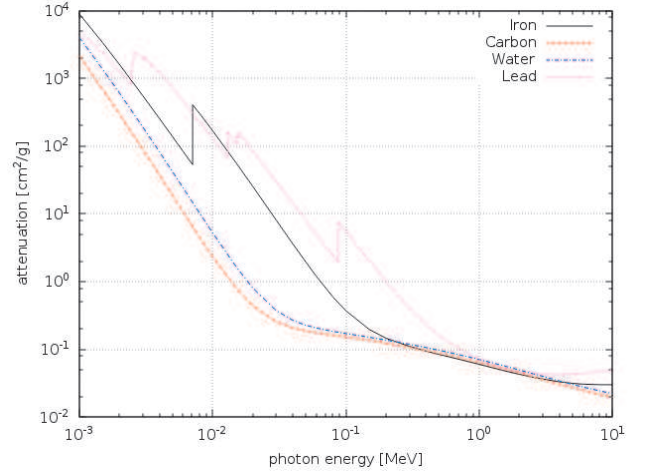

Fig. 2. Dependence between photon energy and attenuation. Values are tabularized, see [7].

our object is not a uniform m_E is:

$$m_E = \sum_{i=0}^{n} -T_i \cdot \rho_i \cdot \tau_i(E, Z_i) \tag{5}$$

where n is number of different materials. N_0 is a variable which depends on photon energy and it will be denoted as $N_0(E)$ from now. Spectra of X-ray is polychromatic, because of that measured energy which has to be distributed in energy range $[E1, E2]$:

$$m_E = -\log\left(\int_{E1}^{E2} N_0'(E) \cdot \exp(-\sum_{i=0}^{n} \rho_i \tau_i(E, Z_i))\right) \tag{6}$$

where $N_0'(E)$ is number of photons emited with energy E in range $[E1, E2]$:

$$N_0'(E) = \frac{D(E) \cdot N_0(E)}{\int_{E1}^{E2} D(E) \cdot N_0(E) \cdot dE} \tag{7}$$

where $D(E)$ represents detector efficiency. The detector efficiency and X-ray tube spectrum are known.

From the equation 6 it could be possible to determine Z value of each material in a scanned object. Unfortunately it is not possible, because of too many variables in this equation. To retrive approximate information of an object material we use combination of data from two measurements of different energies.

We receive number of registered photons that crossed a scanned object (N) from the detector. Knowing the number of photons emitted (N_0) the ratio is given:

$$I(E) = N/N_0 \tag{8}$$

As it was stated in II-A we gather data in two energy ranges, LE and HE, see [8]. Finally, we can use following formulas, to calculate so-called Q values, see [9]:

$$Q = \frac{m_{LE}}{m_{HE}} = \frac{\log I(LE)}{\log I(HE)} \tag{9}$$

Q determines the expected material of and object registered on a pixel and will be used in the proposed algorithm.

III. ALGORITHM

A current section describes a colouring algorithm that uses two raw images received from the scanner to produce equalized and coloured image.

A. Material Determination and Creation of Masks

X-ray images obtained for high energy (HE) and low energy (LE) are shown on figure 3. All image examples in this work are cropped to the region of interest from received scans.
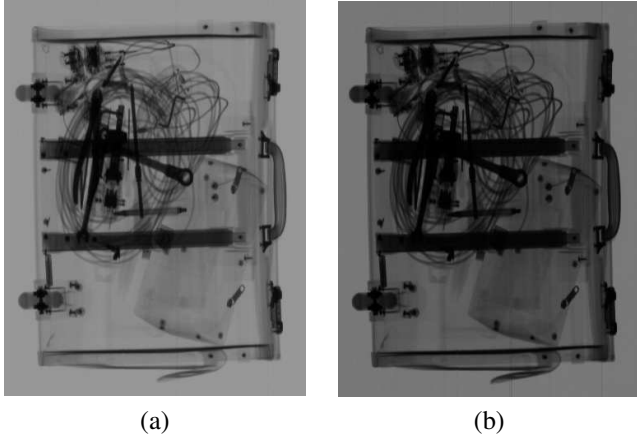
(a) (b)

Fig. 3.   Raw images: (a) high energy, (b) low energy.

In order to determine the Q value we use quotient of the logarithms of object's material values (see Eq. 9) of HE and LE scan. We decided to choose three types of materials depending on the Q value in accordance with the standards used in the professional security scanners:

1) metal – with values between 1.02 – 1.15,
2) plastic – between 1.005 – 1.02,
3) organic – between 0.972 – 1.005.

Pixels with values below 0.972 are treated as a background and pixels with values above 1.15 are marked as not penetrated by X-rays. All of these values were obtained experimentally. These values are tied strictly to the scanner configuration and may vary on different machines and energy settings. After pixel classification we create three binary images representing all types of materials (see Fig. 4).

B. Mask Enhancement

Images generated in such way are very sharp and they have a lot of isolated pixels. Such problem can be fixed by using a morphological filling or blurring. We use a simple Gaussian blurring technic to prepare those images for the next processing step. Optimal sizes of the Gaussian filter masks are 5×5 and 7×7. A filter with a smaller 3×3 mask is unable to cover all in-object holes while bigger masks give no improvement in the final image while increasing computational complexity.

Because of the blurring procedure, the range mask images are overlapping each other nearby edges. We used the Canny edge detection algorithm to restore sharp edges, see [10]. We chose the Canny edge detector due to its ability to describe
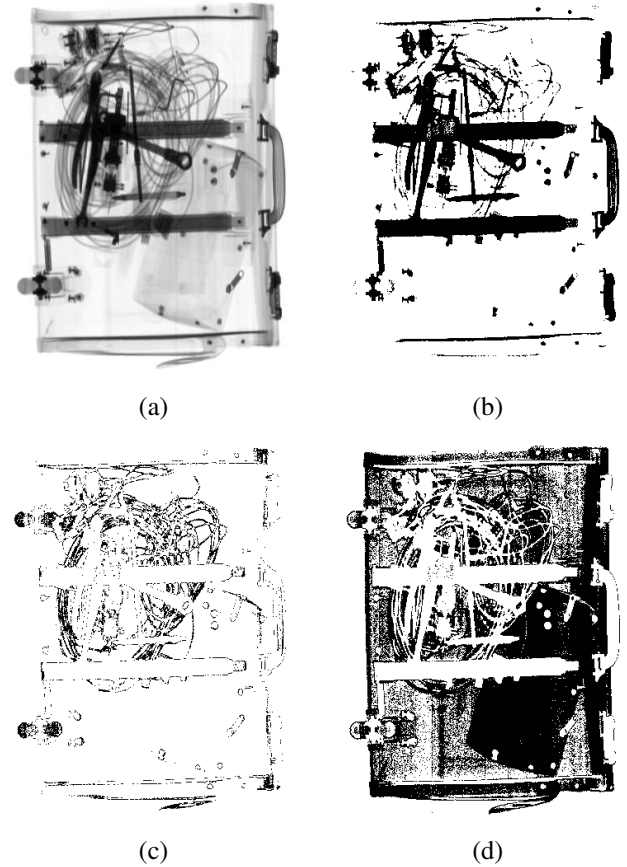
(a) (b)

(c) (d)

Fig. 4.   Material masking: (a) brightness and contrast adjusted raw image (for comparison), (b) metal mask, (c) plastic mask, (d) organic mask.

edges in a vector form. It provides the information about an angle of a contrast gradient in every point classified as the edge.
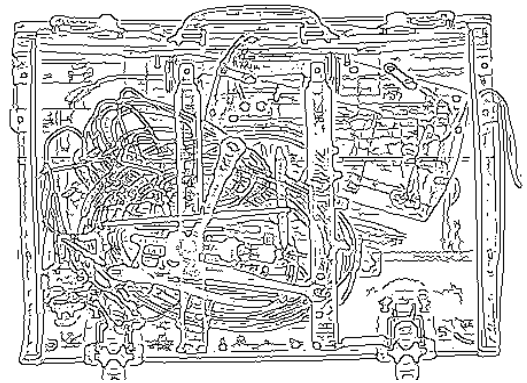
Fig. 5.   An image of edge vectors calculated by the Canny algorithm.

A Sobel filter is used to calculate gradient angles (θ) from horizontal ($\mathbf{G_x}$) and vertical ($\mathbf{G_y}$) direction:

$$\theta = \arctan \frac{\mathbf{G_y}}{\mathbf{G_x}} \qquad (10)$$

These angles are often called contrast gradient degree. In the Canny algorithm, angles are discretized to one of the following

four values (discretized directions θ_D) which are equal to 0, 45, 90 and 135 degrees covering 45 degrees around each one. For every pixel which belongs to Canny's edge vector, the appropriate contrast gradient degree is assigned. We used voting algorithm to determine an affiliation of a point to a certain mask. The size of the region of interest created around current pixel is equal to the size of previously used Gaussian filter mask. An example is shown on Fig. 6.
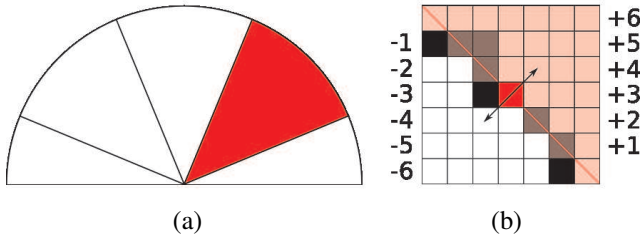

Fig. 6.   Example behavior of an algorithm in case of a pixel with 45 ± 22.5 contrast gradient degree and 7×7 Gaussian mask.

A border found by the Canny algorithm is marked with black pixels. The central red pixel is a border point being processed in the current step. In this example the red pixel has contrast a gradient angle in range of 45 ± 22.5 degrees, so it requires comparision of two neighbouring pixels from SW and NE, which are connected with the arrowed line (see Fig. 6b). Values of these two pixels are read from blurred binary image (see Fig. 7b) and compared which one is greater. Line perpendicular to the proper discretized gradient angle (θ_D) splits the square into two triangles or two rectangles depending on the θ_D. This line is marked as a red line in our example image on Fig. 6b. The triangle (or rectangle) that contains the pixel with higher value is being set as the foreground and the second part of the square is marked as the background. In our example figure the foreground triangle is marked with semitransparent red. These values are used to create so-called affilation matrix which contains information whether the pixel is included in the material layer or not. The affiliation matrix has the same size as the acquired image. Only the pixels that were effectively blurred are being processed this way (see 7c).

Next, the algorithm fills the affiliation mask with the proper values. Every pixel with a maximum value on a blurred image (pure black in Fig. 7b) will be mapped into maximum value on the affiliation mask. Every pixel with a zero value on the same image will be mapped into minimal negative value on the affiliation mask. The values of the other pixels are set to 0 (displayed in a gray in Fig. 7b). At this step, for each pixel in Canny edge vector, the region of interest of the affiliation mask must be determined. This region is centered on the position of the current Canny edge vector pixel. The sizes of this region and Gaussian mask used in previous step are the same. In the region of interest for each foreground pixel positive value is added. This value is proportional to the distance between the point and the borderline separating the foreground and the background parts (red line in Fig. 7b). For each background pixel a negative value is added in the same manner. After the
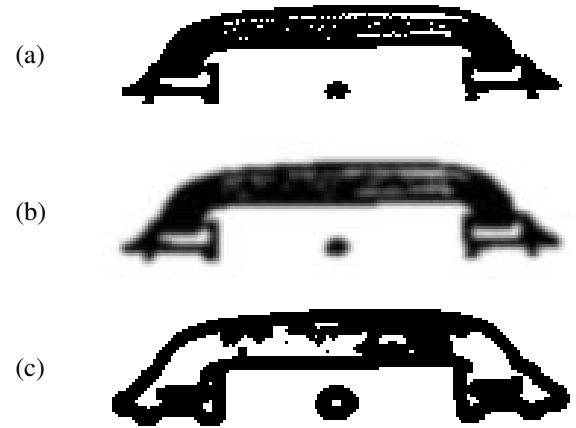

Fig. 7.   Construction of affiliation mask: (a) raw mask, (b) mask blurred using 7×7 Gaussian matrix, (c) affiliation mask containing non-extreme points on (b).

inspection of each edge pixel, all negative pixels are removed from the affiliation mask. It is the final step of the construction of the affiliation mask for the single layer. The affiliation masks must be determined for each material layers.

At this point of analysis there are some pixels that belong to several material layers. We have to determine to which single layer the analyzed pixel should be assigned. We use the voting algorithm which compares affiliation masks pixels from the same coordinates on different material layers. If pixel have maximum value on some mask it's value is not modified, while on the other masks the pixels on the same coordinates are set to zero. Now affiliation mask contains information whether the considered pixel belongs to the specified layer or not. For simplification, this mask is binarized with the threshold level above zero. A final image layer is a bitwise multiplication of the blurred image (Fig. 7b) and the binary affiliation mask. In a last step we colorize the layer mask with predefined hue. We used blue for metal range, orange for plastic range and green for organic – a scheme commonly used in X-ray images pseudocoloring.

C. Histogram Equalization of Background Image

The layer masks are monochromatic. In order to visually separate objects covered by single material layer high contrast background is needed. As it is shown on Fig. 3, raw images are dark and the lack of contrast is visible (especially on LE). For visual inspection of scanned objects we have to prepare images which are displayed with 8-bit depth resolution. Fortunately, the X-ray scanner provides us with 16-bit images, so there is a lot of space to improve visual quality without losing any important information.

Usually scanners produce data recorded in 16-bit grayscale space, but fast inspection of Fig. 8a (see histogram) shows that important information is stored only in a small part of dynamic range. We use histogram normalization for range expansion. Better contrast is achieved by stretching the histogram to use full grayscale space range (see Fig. 8b), see [11].
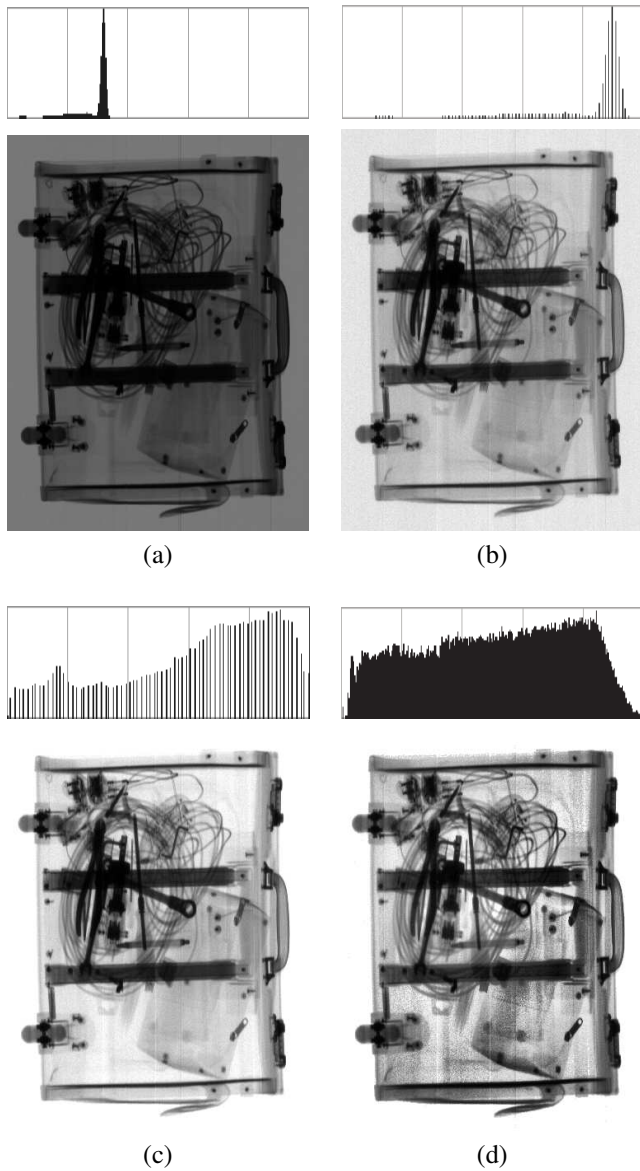
(a)

(b)

(c)

(d)

Fig. 8. Steps of improving background image quality and their histograms: (a) a raw energy image, (b) after normalization, (c) after thresholding (d) after the CLAHE histogram equalization. In (c) and (d) white value is ignored to emphasize rest of histogram. Histograms are displayed for 8-bit images.

Image enchancement is achieved by simple tresholding. Level of threshold is determined as arithmetic mean of background pixel values. For each corner of the image we calculate arithmetic mean of 16×16 pixels. If the difference of mean values between the corners is greater than 10% of depth resolution, then background level is set to 90% of maximum value (for example in 8-bit depth it gives 230). In most cases this value is sufficient to remove all the background noise. For result see Fig. 8c.

Better image contrast can be achieved by using the histogram modification algorithm called CLAHE (Contrast Limited Adaptive Histogram Equalization), see [12]. This algorithm is used for thresholded background. The CLAHE algorithm flattens the histogram in regions where the contrast is high. In regions with low contrast, algorithm increases it. In our case this technics will not reduce information,

because areas with high contrast are additionally distinguished by different color. With help of the CLAHE algorithm it is possible to visulize objects with very low contrast placed on the same material layer. For result see Fig. 8d.

The final step in our algorithm is synthesis of the background and colour material layers.
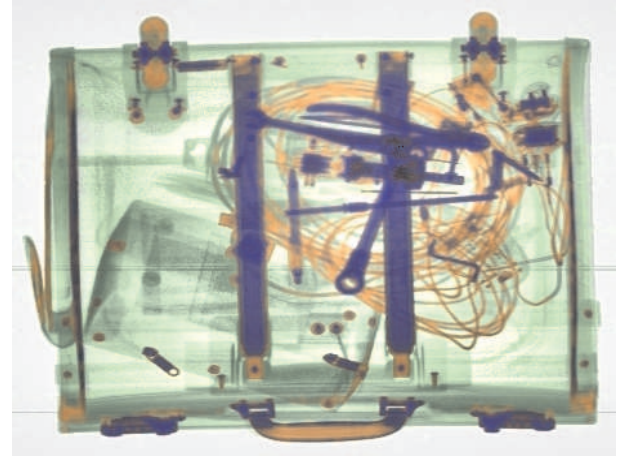

Fig. 9. Result image.

IV. RESULTS

Enhanced colouring algorithm involves the following basic steps:

1) Get high and low energy X-ray images
2) Find binary edges of the high energy image using the Canny algorithm
3) Save values of gradient angles which are co-product of the Canny algorithm
4) Get logarithmized ratio of HE to LE values for every pixel
5) Create n binary images for every material range
6) For each binary image:
   a) Blur image using 5×5 or 7×7 Gaussian filter mask
   b) Create the affiliation mask of sizes equal to binary image
   c) For each egde pixel (found in step 2.):
      i) Determine region of interest on affiliation mask centered in current edge point
      ii) Compare two neighbour pixels placed along line determined by gradient angle
      iii) Set perpendicular to this line splitting its neighbourhood into foreground and background parts
      iv) For each pixel in region of interest:
         If pixel lies in foreground part:
            pixel gets affiliation values added
         else:
            pixel gets affiliation values subtracted
   d) Remove any negative values from affiliation mask.

7) Determinate affiliation masks choosing pixels with maximum values.
8) Binarize affiliation masks
9) For each binary image:
    a) Multiply Gaussian blurred binary image with corresponding affiliation mask
    b) Set colour creating final material layer
10) Normalize the contrast of high energy image
11) Adjust image threshold
12) Apply CLAHE filter creating final background image
13) Place each material layer on background image.

The most important benefit of presented algorithm is an ability to distinguish between material layers regardless of whether the edges of scanned object are smooth or sharp. The described algorithm can analyze unrestricted number of different layers. We have to remember that in practical scanning baggage procedure, inspectors can be confused seeing more than 4 different colour ranges.

Algorithm's time computational complexity is polynomial and depends on the number of layers' edge pixels. Presented algorithm runs almost real time on our testing machine with Intel i5-3470 3.2 GHz. Processing time for the single scan image with resolution 1024×1024 pixels vary between 1 and 3 seconds for typical scanned object. Such processing time is shorter than time needed for the scanner user needs to complete the operating task.

V. CONCLUSION

The discussed false colouring algorithm has already been introduced into proffesional usage as a part of a software driver for scanners produced under the name of "Arida". It is being used among others image adjusting and object detection algorithms. A coloured X-ray image is a basic tool for baggage iscpectors.

This algorithm is also used for potential risk detection filter where areas of attenuation coefficient are close to known drugs and explosives.

In the current state of the project the false coloring algorithm is no logner part of active development as it satisfies an scanner customers. Currently our team works on an algorithm for risk detection based on both material properties and on geometric information like for example the shape a weapon, see [13].

REFERENCES

[1] K. Moreland, "Diverging color maps for scientific visualization," *Advances in Visual Computing*, pp. 92–103, 2009.
[2] G. Flitton, T. Breckon, and N. Megherbi, "A comparison of 3d interest point descriptors with application to airport baggage object detection in complex ct imagery." *Pattern Recognition*, vol. 46, pp. 2420–2436, 2013.
[3] Z. Ying, R. Naidu, and C. Crowford, "Dual energy computed tomography for explosive detection," *Journal of X-Ray Science and Technology*, vol. 14, pp. 235–256, 2006.
[4] H. Watabiki, T. Takeda, M. S., and Y. T., "Development of dual-energy x-ray inspection system," *Anritsu Technical Review*, vol. 20, pp. 59–66, 2013.
[5] J. Evans, Y. Liu, J. Chan, and D. Downes, "View synthesis for depth from motion 3d x-ray imaging." *Pattern Recognition Letters*, vol. 44, pp. 1863–1873, 2006.
[6] V. Rebuffel and J. Dinten, "Dual-energy x-ray imaging: Benefits and limits," *ECNDT*, vol. 1.3.1., 2006.
[7] J. Hubbell and S. Seltzer, "Tables of x-ray mass attenuation coefficients and mass energy-absorption coefficients from 1 kev to 20 mev for elements z = 1 to 92 and 48 additional substances of dosimetric interest," *NISTIR*, vol. 5632, 1995.
[8] S. Chang, H. Lee, and G. Cho, "Application of a dual-energy monochromatic x-ray ct algorithm to polychromatic x-ray ct: a feasibility study," *Nuclear Engineering Technology*, vol. 44, pp. 61–70, 2012.
[9] F. Firsching, T. Fuchs, and N. Uhlmann, "Method for dual high energy x-ray imaging with flat panel detectors," *ECNDT*, vol. 1.3.1., 2006.
[10] J. Parker, *Algorithms for Image Processing and Computer Vision*. Wiley, 1997.
[11] S. Khan and W. Chai, "An image enhancement technique of x-ray carry on luggage for detection of contraband/illicit object(s)." *IJCSI International Journal of Computer Science Issues*, vol. 9, pp. 205–211, 2012.
[12] K. Zuiderveld, "Contrast limited adaptive histogram equalization," in *Graphics gems IV*, P. Heckbert, Ed. San Diego: Academic Press Professional, 1994, pp. 474–485.
[13] M. Roomi and R. Rajashankarii, "Detection of concealed weapons in x-ray images using fuzzy k-nn." *International Journal of Computer Science, Engineering and Information Technology*, vol. 2, pp. 187–196, 2012.